Supporting Information

Molecular Wrench Activity of DNA Helicases: Keys to Modulation of Rapid Kinetics in DNA Repair

Ashan Wettasinghe,[1] Melodee O. Seifi,[1] Marco Bravo,[2] Austen C. Adams,[1] Aman Patel,[1] Monica Lou,[1] Dimithree Kahanda,[1] Hao-Che Peng,[3] Allison L. Stelling,[3] Li Fan,[3] and Jason D. Slinker[1,3,4*]*

[1]Department of Physics, The University of Texas at Dallas, 800 W. Campbell Rd., SCI 10, Richardson, TX 75080.

[2]Department of Biochemistry, University of California, 900 University Ave, Riverside, CA 92521.

[3]Department of Chemistry, The University of Texas at Dallas, 800 W. Campbell Rd., SCI 10, Richardson, TX 75080.

[4]Department of Materials Science and Engineering, The University of Texas at Dallas, 800 W. Campbell Rd., SCI10, Richardson, TX 75080

Corresponding authors:

*Li Fan, Department of Biochemistry, University of California, 900 University Ave, Riverside, CA 92521. Phone: 951-827-3630. Fax: 951-827-4434. E-mail: li.fan@ucr.edu.

*Jason Slinker, The University of Texas at Dallas, 800 W. Campbell Rd., SCI 10, Richardson, TX 75080. Phone: 972-883-6513. Fax: 972-883-2848. E-mail: slinker@utdallas.edu.

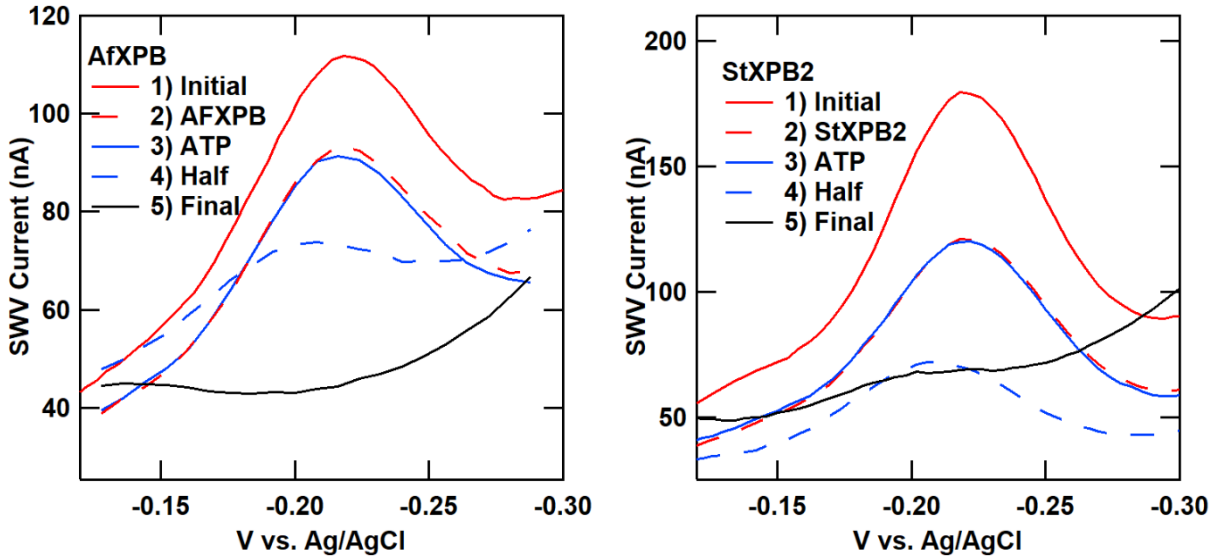

Figure S1. Example SWV curves for AFXPB (40 nM) and StXPB2 (200 nM) experiments. 1) Initial SWV curve of Nile blue modified DNA monolayer electrochemistry. 2) Equilibrated SWV curve after the addition of helicase. 3) SWV immediately after adding 2 mM ATP into the helicase-incubated solution. 4) SWV after half of the signal has decayed following ATP addition into the helicase-incubated solution. 5) SWV at the final state after ATP addition into the helicase-incubated solution.

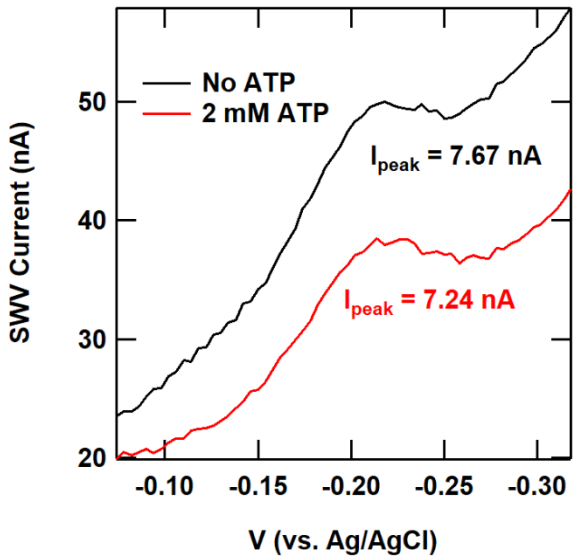

Figure S2. Control experiment for ATP addition. (Black "No ATP" curve) Initial SWV curve of Nile blue modified DNA monolayer electrochemistry. (Red "2 mM ATP" curve) Final SWV curve after successive additions of ATP to equilibrate a final concentration of 2mM.

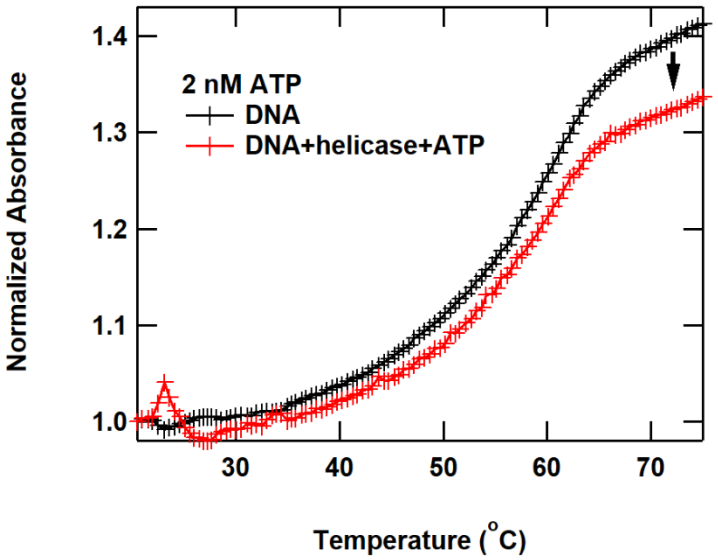

Figure S3. Control UV-Visible spectrometry experiment for ATP-induced DNA unzipping by helicases. Normalized absorbance at 260 nm versus temperature for duplex DNA (309 nM) and duplex DNA mixed with 40 nM AfXPB helicase and 2 nM ATP.

DNA experiences hyperchromicity, increasing absorbance when heated through the melting temperature as the duplex splits into two individual strands. A lowered change in absorbance is evidence of DNA dehybridization by helicase activity.

Helicase	Concentration	τ(s)	Notes
StXPB2	8 nM	5000 ± 1000	
StXPB2	200 nM	2900 ± 500	
StXPB2-Bax1	10 nM	3330 ± 70	
StXPB2-Bax1	200 nM	7.1 ± 0.8	
AfXPB	8 nM	2400 ± 800	
AfXPB	20 nM	6.2 ± 0.8 1600 ± 100	Linear recovery between exponential decays with a slope m = 1.1 ± 0.2 %/s
AfXPB	40 nM	7.0 ± 0.5	
AfXPB	200 nM	4 ± 2	
AfXPB-Bax1	10 nM	4200 ± 400	
AfXPB-Bax1	200 nM	3500 ± 500	

Table S1. Summarized time constants for exponential SWV peak current decay for StXPB2 and AfXPB helicases and associated helicase-Bax1 complexes at various concentrations.

Helicase	K_{D1} (nM)	K_{D2} (nM)	Fit
StXPB2	158		Hill equation with n = 1.43
StXPB2-Bax1	640		Langmuir binding isotherm
AfXPB	25	334	Two Langmuir binding isotherms
AfXPB-Bax1	145		Hill equation with n = 2.2

Table S2. Summarized binding dissociation constants for StXPB2 and AfXPB helicases and associated helicase-Bax1 complexes.

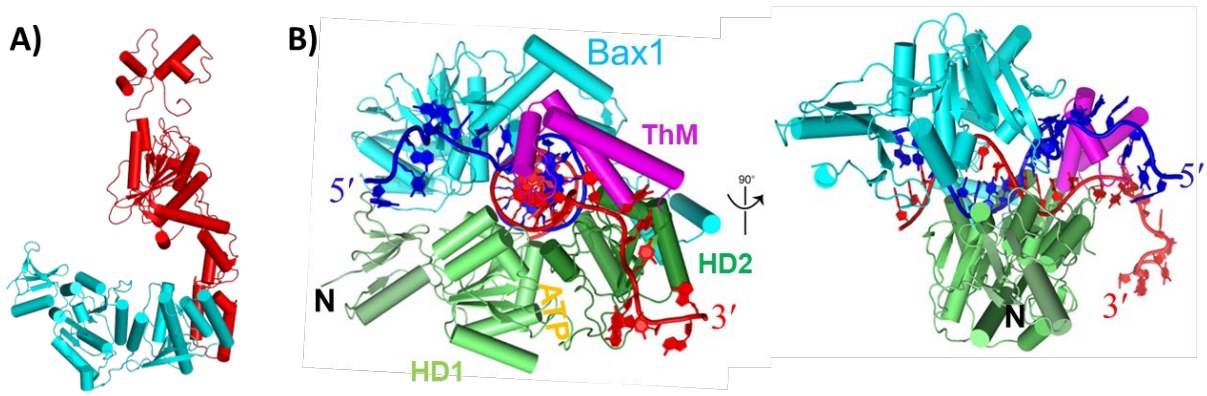

Figure S4. StXPB Bax1 crystal structures. A) StXPB2-Bax1 complex (6P4O.pdb) StXPB2 (cyan) is in the closed conformation. B) The ternary structure of the StXPB2-Bax1-DNA complex (6P4F.pdb, NAR 2020). StXPB2 in the closed conformation.

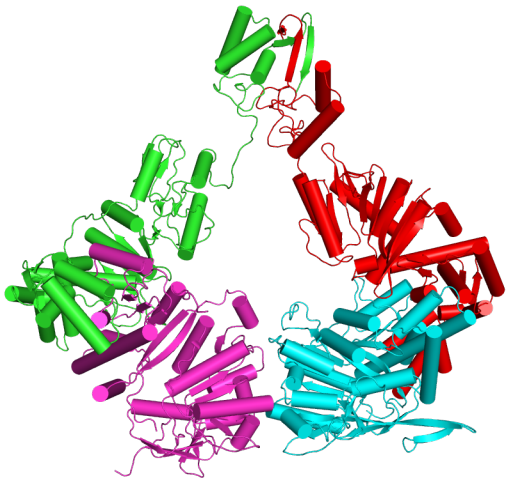

Figure S5. Dimer of the AfXPB-Bax1 complex in crystal (6P66.pdb). AfXPB is in the open conformation (magenta & cyan). Dimerization is likely at high concentrations, which may inhibit ATP binding.

Investigation of Rapid Reactions with Intrasweep Square Wave Voltammetry (ISWV)

Surface-bound electrochemistry is useful for measuring and physically characterizing the reactions of molecules related to biology, chemistry, energy, and the environment.[1] Among electrochemical techniques applied at surfaces, square wave voltammetry (SWV) is particularly attractive.[2] The square wave voltammetric waveform combines a modulated large-amplitude square wave with a staircase potential. Current is measured twice within each period of the square wave, at the ends of the forward and reverse pulses, and these sampled currents are subtracted from each other to yield a truly differential measurement. The resulting current tends to cancel out capacitive or non-faradaic currents while enhancing electronic or faradaic currents. As a result, SWV is highly beneficial for electrochemical measurements in complex environments where electronic current information is desired in an ionically conducting environment.

The measurement time t of a conventional SWV waveform is determined by

$$t = \tau\left(\frac{\Delta E_w}{\Delta E_s}\right) \quad \text{(Equation S1)}$$

where τ is the measurement period, ΔE_w is the potential range of the full SWV waveform, and ΔE_s is the step height of the staircase potential. Measurements can be taken rapidly if the frequency of the waveform is high. This frequency is ultimately determined by the electron transfer rate, k_{et}, of the electrochemical reaction. A maximal reversible square wave signal is observed when the electron transfer rate is balanced with the SWV frequency, i.e., $k_{et}\tau = 1$. If successive SWV measurements are used to obtain the kinetics of a secondary reaction, then the time resolution of the measurement is set by the t of Equation S1. However, if this secondary reaction proceeds on a timescale shorter than t, the detailed kinetics of the reaction are lost.

Several electrochemical approaches have described techniques to obtain high temporal resolution. In particular, rapid cyclic voltammetry, chronoamperometry, and intermittent pulse voltammetry have been used to obtain millisecond time scales of biological reactions.[3-6] However, in general, these have not leveraged the chief advantage of SWV—the rejection of background capacitive currents, which may be present in chemical reactions with a high concentration of mobile ions. Here, we describe a straightforward means of improving the temporal resolution of the chemical reaction measurements from t to τ, a general factor of $\Delta E_w/\Delta E_s$ corresponding to the number of points of the sweep. This is accomplished by performing this chemical reaction within the sweep of SWV and is termed intrasweep square wave voltammetry (ISWV). This technique is demonstrated with the rapid degradation of an electrochemically-active double-stranded DNA monolayer under acid conditions.

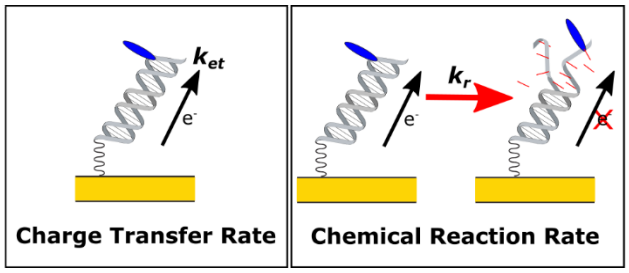

Figure S6. Illustration of the Nile blue modified DNA monolayers used for study, the electron transfer reaction (k_{et}), and dehybridizing chemical reaction (k_r).

To demonstrate the technique of an ISWV approach for obtaining the kinetics of a rapid chemical reaction (k_r), we utilized double-stranded 17-mer DNA monolayers modified with an electrochemically active Nile Blue redox probe. (Figure S6) These monolayers were assembled on gold electrodes on multiplexed chips, and electrochemical reactions were driven with reference and counter electrodes suspended in solution over the devices. Under these conditions, we have generally measured the electron transfer rate k_{et} to be on the order of 1-10 s^{-1},[7-11] and numerical fitting of an example curve as previously described[8-9] reveals a $k_{et} = 1.2\ s^{-1}$. The solution can rapidly transition from biologically stable pH to acidic conditions by adding adenosine triphosphate (ATP) into a low-capacity buffer solution. Double-stranded DNA monolayers rapidly undergo depurination under these conditions,[12] which quickly dehybridizes the DNA duplex—splitting the double-stranded DNA into individual strands. This causes rapid loss of the electrochemical signal, consistent with many previous reports of induced dehybridization.[7-10]

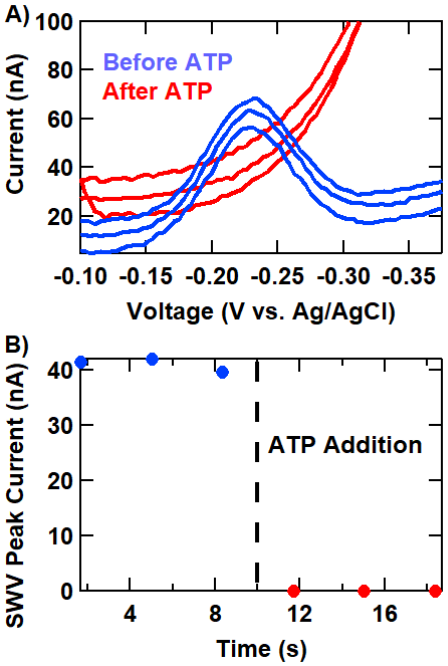

Figure S7. ATP-driven chemical reaction kinetic analysis by conventional SWV. A) Successive SWV curves obtained before and after 2mM ATP addition. B) Square wave peak current versus time.

To perform conventional SWV kinetic analysis, we used a modest potential sweep spanning 280 mV at 60 Hz and minimal instrumental time between measurements. This leads to successive measurements that are 3.34 s apart. Thus, this sets the time scale of the resolution of measurements for a kinetics approach using conventional successive waveforms of square wave voltammetry with this system. Increasing the frequency beyond 60 Hz for this system leads to significantly lower peak currents and loss of signal-to-noise.

The results of this conventional SWV approach are shown in Figure S7. Successive SWV curves before and after ATP addition are shown in Figure S5A. Before ATP addition, a significant redox peak current of 37.5 nA is located at −0.22 V vs. Ag/AgCl, associated with the reduction of the Nile Blue probe coupled to undamaged DNA. Upon the addition of 2mM ATP between SWV measurements, this peak current is completely eliminated. Under these conditions, the concentration of ATP molecules surpasses the buffer chemicals and turns the solution acidic. Due to these acidic conditions, the base pairing of the DNA is lost due to depurination, leading to DNA dehybridization that decreases the electrochemical signal. (Subsequently, the exposed gold electrode leads to high background current, partly due to irreversible oxygen electrochemistry.) Figure S5B summarizes the SWV peak current versus time for these three successive runs taken immediately before and immediately after ATP addition. All singals due to the reaction kinetics are lost due to the rapid rate of the degradation reaction.

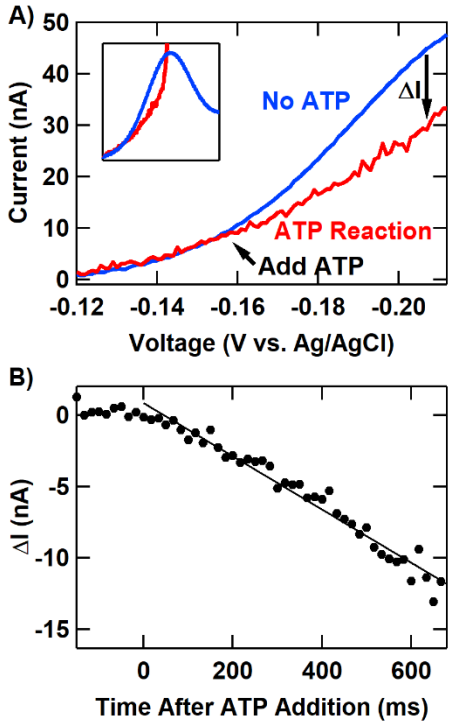

Figure S8. ATP-driven chemical reaction kinetic analysis by ISWV. A) Averaged SWV curve before ATP addition (25 curve average, blue) and SWV curve upon adding ATP during the sweep (red) from −0.12 V to −0.212 V vs. Ag/AgCl. The inset shows the full range from −0.12 to −0.30 V. B) The difference current ΔI between the two curves of Figure S6A (ISWV difference curve) plotted versus time after ATP addition.

In Figure S8, we present the results of using the ISWV approach. Initially, several SWV sweeps are recorded before the chemical reaction is initiated to establish a clear pre-reaction curve that limits noise contributions. We recorded 25 SWV sweeps and present the full average curve in the inset in Figure S8A. Subsequently, the ATP-driven chemical reaction is initiated *during* a conventional SWV sweep, in this case, just at the initial rise of the SWV curve. The chemical reaction is commenced during the SWV sweep for an intrasweep reaction. After correcting for a constant background difference, the difference in current between the pre-reaction averaged curve (Figure S8A, blue curve) and the active reaction curve (Figure S8A, red curve) is then recorded as the change in current ΔI.

In Figure S8B, this difference in current between pre-reaction and active reaction curves ΔI is plotted versus time after ATP addition. (The first 2/3 s are plotted as the monolayer is lost, and the signal rapidly increases after this time.) The conversion from voltage to time is straightforward as each point is a SWV period apart, in this case, 1/60 s or 16.7 ms. The change in current reveals the reaction kinetics of the loss of electrochemical signal from the degradation of the monolayer. The curve is well fit with a line (R^2=0.968) having a slope of 18.6 pA/ms, or 49% of the peak current per second. In recording this way, the time resolution is improved from 3.34 s for the conventional measurement to 16.7 ms for the ISWV measurement, an improvement by a factor of 200. Note that the slope observed corresponds to a SWV peak current loss of 49% per second, well beyond the resolving capacity of the conventional SWV technique. Furthermore, this system is difficult to follow with a standard linear technique. The background current of the forward sweep of the SWV curve increases from 2.5 nA before the addition of ATP to a nonlinear current as high as 60 nA after the addition of ATP. The SWV measurement effectively removes these background changes.

Overall, intrasweep square wave voltammetry is a generalizable means to leverage square wave voltammetry to analyze chemical reactions with fast kinetic processes. The ISWV approach is particularly beneficial for analyzing chemical reactions approaching the rate of electron transfer of the redox system. To apply this technique in general, it is ideal to initiate the chemical reaction within the redox peak of the ISWV measurement. This ensures a high faradaic current that provides a large current change for high signal-to-noise. Recording conventional SWV curves before initiating the reaction also improves results by minimizing the noise of the pre-reaction curve.

Experimental Section for ISWV experiment

DNA. Double-stranded DNA was prepared using the 17mer sequence 3'-CTCTATATTTCGTGCGT$_{NB}$-5' and its complementary sequence 5'-(C6 thiol)-GAGATATAAAGCACGCA-3'. T_{NB} denotes the position of the thymine modified with a Nile Blue redox probe, and C6 thiol is the Glen Research thiol-modifier C6 S-S phosphoramidite. The DNA modified with the Nile blue (NB) precursor base, a 5-[3-acrylate NHS ester] deoxyuridine phosphoramidite derived by Glen Research, was purchased from Trilink BioTechnologies. The dye was covalently coupled under ultramild conditions according to established procedures.[11] Thiolated DNA sequences were obtained from Integrated DNA Technologies (IDT).

Purification of DNA. All oligonucleotides were purified *via* two rounds of high-performance liquid chromatography (HPLC) on a Shimadzu LC-20AD instrument outfitted with a SIL-20A

autosampler and an SPD-M20A diode array detector. In the first purification round, DNA oligonucleotides with the 4,4′-dimethoxytrityl group on were eluted on a gradient that was evolved from 5% acetonitrile and 95% 50 mM ammonium acetate, pH = 8 buffer to 75% acetonitrile and 25% 50 mM ammonium acetate, pH = 8 buffer over 30 min. In the second purification round, DNA oligonucleotides with the 4,4′-dimethoxytrityl group off were eluted on a gradient that was evolved from 5% acetonitrile and 95% 50 mM ammonium acetate, pH = 8 buffer to 15% acetonitrile and 85% 50 mM ammonium acetate, pH = 8 buffer over the first 35 min; from 15% acetonitrile and 85% 50 mM ammonium acetate, pH = 8 buffer to 50% acetonitrile and 50% 50 mM ammonium acetate, pH = 8 buffer over the next 5 min; and finally, held constant at 50% acetonitrile for another 5 min. The identity of the desired products was confirmed by matrix-assisted laser desorption ionization time-of-flight mass spectrometry (MALDI-TOF) on a Shimadzu Axima Confidence mass spectrometer.

Preparation of the double-stranded DNA. The oligonucleotides were quantified *via* UV-visible spectroscopy on a Beckman DU-800 UV-Visible spectrophotometer. Next, duplex DNA was prepared by mixing equimolar amounts of complementary strands and annealing the solution to 95 °C, followed by slow cooling to room temperature over a period of 90 min. The formation of duplex DNA was verified by UV melting temperature analysis.

Fabrication of Devices. The chips/substrates featuring multiplexed gold electrodes for DNA self-assembly and electrochemical experiments were prepared as previously described.[7]

Self-Assembly of DNA Monolayers. The DNA monolayers were self-assembled onto gold electrode pads from a solution with 25 μM of the duplex DNA, 5 mM phosphate, 50 mM sodium chloride, pH = 7 buffer solution over 12 h to 18 h. The substrates were backfilled with mercaptohexanol for 1 h to remove nonspecifically bound DNA and then thoroughly rinsed with buffer to remove residual mercaptohexanol.

Electrochemical measurements on DNA monolayers. The multiplexed substrates were placed in a custom mount[10] and connected to electrochemical testing hardware (a CH Instruments CHI750D Electrochemical Analyzer and a CHI 684 Multiplexer). Square wave voltammetry was generally performed at 60 Hz with a 0.025 mV amplitude and 1 mV increment. The electrochemical measurements were performed in a buffer containing 50 mM NaCl, 10 mM Tris-HCl, 10 mM $MgCl_2$, and 4 mM spermidine.

Supplementary Materials References

1. Eckermann, A. L.; Feld, D. J.; Shaw, J. A.; Meade, T. J., Electrochemistry of redox-active self-assembled monolayers. *Coord. Chem. Rev.* **2010,** *254* (15-16), 1769-1802.
2. Osteryoung, J. G.; Osteryoung, R. A., Square-Wave Voltammetry. *Anal. Chem.* **1985,** *57* (1), 101-110.
3. Arroyo-Curras, N.; Dauphin-Ducharme, P.; Ortega, G.; Ploense, K. L.; Kippin, T. E.; Plaxco, K. W., Subsecond-Resolved Molecular Measurements in the Living Body Using Chronoamperometrically Interrogated Aptamer-Based Sensors. *ACS Sens.* **2018,** *3* (2), 360-366.

4. Santos-Cancel, M.; Lazenby, R. A.; White, R. J., Rapid Two-Millisecond Interrogation of Electrochemical, Aptamer-Based Sensor Response Using Intermittent Pulse Amperometry. *ACS Sens.* **2018,** *3* (6), 1203-1209.
5. Heien, M.; Johnson, M. A.; Wightman, R. M., Resolving neurotransmitters detected by fast-scan cyclic voltammetry. *Anal. Chem.* **2004,** *76* (19), 5697-5704.
6. Weber, K.; Creager, S. E., Voltammetry of Redox-Active Groups Irreversibly Adsorbed Onto Electrodes--Treatment Using the Marcus Relation Between Rate and Overpotential. *Anal. Chem.* **1994,** *66* (19), 3164-3172.
7. Wohlgamuth, C. H.; McWilliams, M. A.; Mazaheripour, A.; Burke, A. M.; Lin, K. Y.; Doan, L.; Slinker, J. D.; Gorodetsky, A. A., Electrochemistry of DNA Mono layers Modified With a Perylenediimide Base Surrogate. *J. Phys. Chem. C* **2014,** *118* (50), 29084-29090.
8. McWilliams, M. A.; Bhui, R.; Taylor, D. W.; Slinker, J. D., The Electronic Influence of Abasic Sites in DNA. *J. Am. Chem. Soc.* **2015,** *137*, 11150–11155.
9. Wohlgamuth, C. H.; McWilliams, M. A.; Slinker, J. D., DNA as a Molecular Wire: Distance and Sequence Dependence. *Anal. Chem.* **2013,** *85* (18), 8634-8640.
10. Wohlgamuth, C. H.; McWilliams, M. A.; Slinker, J. D., Temperature Dependence of Electrochemical DNA Charge Transport: Influence of a Mismatch. *Anal. Chem.* **2013,** *85* (3), 1462-1467.
11. Slinker, J. D.; Muren, N. B.; Gorodetsky, A. A.; Barton, J. K., Multiplexed DNA-Modified Electrodes. *J. Am. Chem. Soc.* **2010,** *132* (8), 2769-2774.
12. Hodes, M. E.; Chargaff, E., The Apurinic Acids from Deoxyribonucleic Acid Fractions. *Biochim. Biophys. Acta* **1956,** *22* (2), 348-360.